DALTON
FULL PAPER

Redox and photochemical behaviour of ruthenium(II) complexes with H_2dcbpy ligand (H_2dcbpy = 2,2′-bipyridine-4,4′-dicarboxylic acid)

Esa Eskelinen, Saija Luukkanen, Matti Haukka, Markku Ahlgrén and Tapani A. Pakkanen *

Department of Chemistry, University of Joensuu, P.O. Box 111, FIN-80101 Joensuu, Finland.
E-mail: Tapani.Pakkanen@joensuu.fi; Fax: +358-13-2513344

Received 6th January 2000, Accepted 19th June 2000
Published on the Web 24th July 2000

The electrochemical redox properties of the ruthenium(II) complexes $Ru(H_2dcbpy)(CO)_2Cl_2$ **1**, $Ru(H_2dcbpy)_2Cl_2$ **2**, $Ru(H_2dcbpy)_2Br_2$ **3**, $Ru(H_2dcbpy)_2(dcbpy)$ **4** and $[Ru(H_2dcbpy)_3]Cl_2$ **5** [H_2dcbpy = 2,2′-bipyridine-4,4′-dicarboxylic acid] were studied in CH_3CN and DMSO by cyclic voltammetry. The metal-based Ru^{II}–Ru^{III} oxidations are observed at variable positive potentials ($E_{1/2}$ = 0.15–1.62 V *vs.* Ag^+–Ag). The H_2dcbpy ligands withdraw electron density from the ruthenium centre and make the oxidation more difficult (seen as positive shifts in $E_{1/2}$ values). At negative potentials the first irreversible ligand-based reductions (E_{pc} = −1.37 to −1.57 V) are due to the deprotonation of carboxylic acid groups whereas the subsequent reversible reactions at high negative potentials are assigned as bipyridine ring based reductions. Based on CV and UV-Vis studies, photoirradiation in the co-ordinating solvent (CH_3CN) revealed the tendency to light-induced CH_3CN co-ordination for complexes **1**–**5**. The photochemical products were also identified by using Lever's *E*(L) parameters. For example, upon photoirradiation of **1**, the principal product is $Ru(H_2dcbpy)(CO)(CH_3CN)Cl_2$. The structures of **1** and **3**–**5** were determined by single-crystal X-ray crystallography.

Introduction

Ruthenium(II) forms with 2,2′-bipyridine (bpy) and its derivatives a large number of mononuclear mono, bis and tris complexes. The vast majority of studies have focused on bis and tris complexes. Interest in the latter has been stimulated by their light-induced electron and energy transfer properties and the various applications utilising these phenomena.[1] The structural influence on the electrochemical properties of these compounds has extensively been studied. The effects of different ligands on ruthenium based redox reactions are well known[2] and several equations have been presented to correlate Ru^{III}–Ru^{II} oxidation potentials with bipyridine based (bpy–bpy^-) reduction potentials.[3] The electrochemical behaviour of corresponding mono complexes have attracted less attention. It was found in earlier studies[4] that the $Ru(bpy)(CO)_2Cl_2$ type complexes act as notable catalysts in electrochemical reduction of CO_2 and just recently[5] structurally related complexes have electrochemically been characterised.

The photochemical reactivity of ruthenium(II) poly(bipyridines) has extensively been studied. Again, $Ru(bpy)_3^{2+}$ and its derivatives have been under careful investigations.[6] Light-induced electron transfer reactions and comparatively long-lived excited states among other features have led to explorations of the ground and excited states of these molecules.[7] Photoinduced substitution reactions of ruthenium tris[8] and bis[9] complexes have widely been studied since the 1980s. It is clear that photoirradiation involves loss of the monodentate ligands and even the bidentate bpy ligands, which are then substituted with co-ordinating solvent molecules, added anions or counter ions. These photoreactions have been exploited in finding synthetic routes to substituted ruthenium bipyridine complexes.[10] Photoirradiation of $Ru(bpy)(CO)_2Cl_2$ in the co-ordinating solvent CH_3CN resulted in multistep substitution of CO and Cl ligands by solvent.[11] In the poorly co-ordinating solvent CH_2Cl_2 irradiation led to dimeric ruthenium(II) complexes, $[Ru(bpy)(CO)Cl_2]_2$.[12]

We have earlier synthesized several ruthenium(II) carbonyl mono(L) type complexes $Ru(L)(CO)_2X_2$; L = 2,2′-bipyridine, 4,4′- or 6,6′-dimethyl-2,2′-bipyridine; X = Cl, Br, I or SCN.[13] These complexes represent potential starting materials for ligand exchange and modification reactions brought about either chemically or *via* photolysis.[11] We have now extended our synthetic methods to H_2dcbpy (2,2′-bipyridine-4,4′-dicarboxylic acid) complexes. As a result, we report here cyclic voltammetric studies of five ruthenium(II) mono-, bis- and tris-(H_2dcbpy) complexes, $Ru(H_2dcbpy)(CO)_2Cl_2$ **1**, *cis*-$Ru(H_2dcbpy)_2Cl_2$ **2**, *cis*-$Ru(H_2dcbpy)_2Br_2$ **3**, $Ru(H_2dcbpy)_2(dcbpy)$ **4** and $[Ru(H_2dcbpy)_3]Cl_2$ **5**. We have also included the photochemical behaviour of these complexes in order to study the possible light-induced ligand substitution reactions, which can be followed by cyclic voltammetry and UV-Vis spectroscopy.[11] Only few ruthenium(II) 2,2′-bipyridine-4,4′-dicarboxylic acid complexes have been characterised by single-crystal X-ray diffraction measurements. Examples of these are $Ru(H_2dcbpy)Cl_3(NO)$[14] and $Ru(dcbpy)_2(NCS)_2$.[15] We present herein the crystal structures of complexes **1** and **3**–**5**.

Results and discussion

Syntheses and structural characterisations

The studied ruthenium(II) complexes containing H_2dcbpy ligands were synthesized in pressure vessels to improve the solubility of the ligand. Similar experimental procedures have been used earlier to prepare ruthenium(II) mono(L) complexes, where L = bpy, dmbpy (4,4′-dimethyl-2,2′-bipyridine) or H_2dcbpy.[13b,c,14,16,17] We have now utilised this synthetic procedure in the preparation of ruthenium(II) bis- and tris-(H_2dcbpy) complexes.

The co-ordination geometry of Ru in all complexes **1** and **3**–**5** was octahedral (Figs. 1–3, Tables 1, 2). The bond lengths and angles are typical for this type of compound.[13a,14,16] The *trans* weakening effect of CO can be seen in **1** where the Ru(1)–Cl(1)

DOI: 10.1039/b004751l

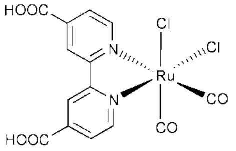

1

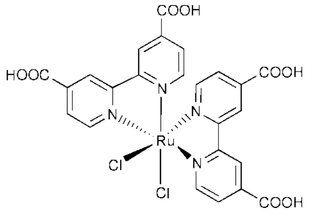

2

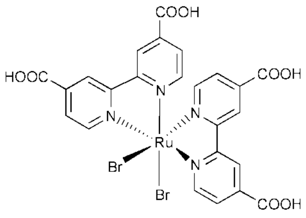

3

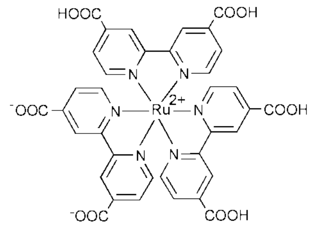

4

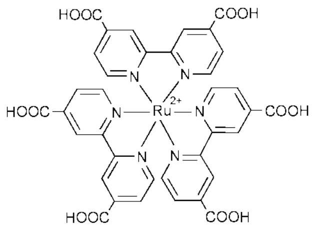

5

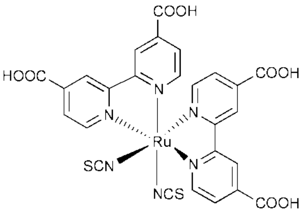

6

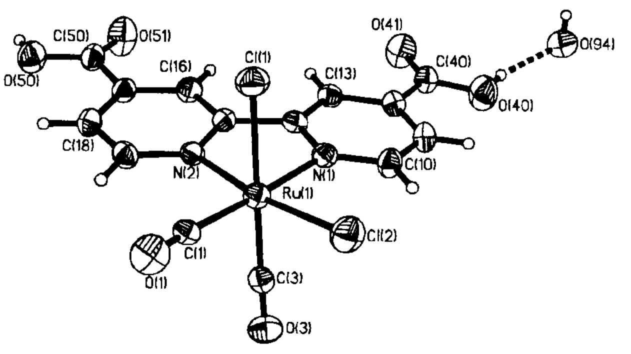

Fig. 1 Crystal structure of $Ru(H_2dcbpy)(CO)_2Cl_2$ **1**.

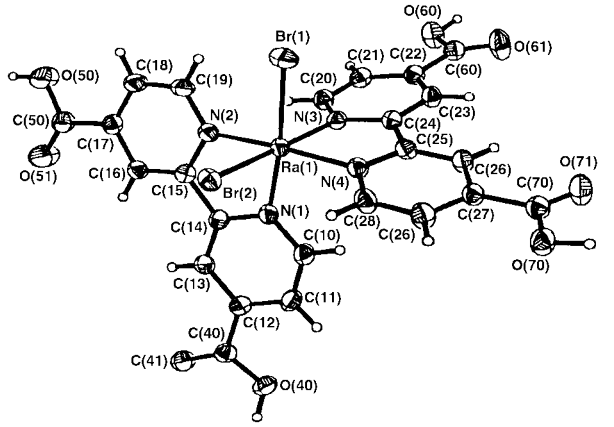

Fig. 2 Crystal structure of $Ru(H_2dcbpy)_2Br_2$ **3**.

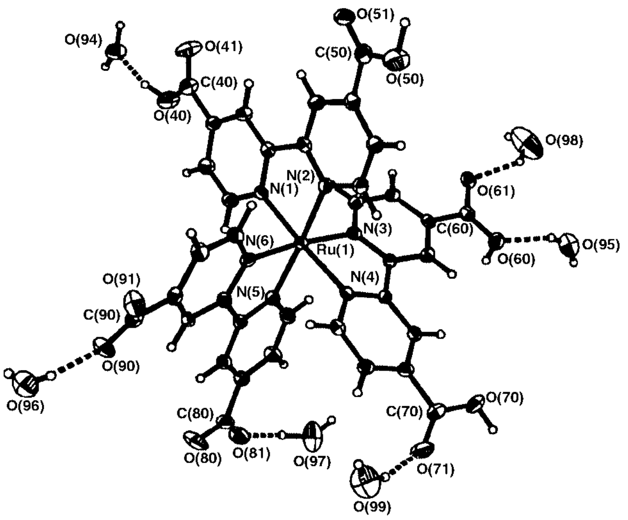

Fig. 3 Crystal structure of $Ru(H_2dcbpy)_2(dcbpy)$ **4**.

bond *trans* to CO (2.4205(11) Å) is slightly longer than the corresponding Ru(1)–Cl(2) bond *trans* to bipyridine nitrogen (2.3722(11) Å). The Ru(1)–C(1) bond *trans* to N(1) is elongated (1.937(5) Å) compared to Ru(1)–C(3) *trans* to Cl(1) (1.873(5) Å). Similar elongation has been observed in *cis*(CO),*cis*(Cl)–$Ru(bpy)(CO)_2Cl_2$.[13a] The co-ordination sphere of Ru is essentially the same in both tris H_2dcbpy compounds **4** and **5** (Tables 1 and 2). Protonation of carboxylate (dcbpy) groups has practically no effects on the bond lengths to Ru.

Cyclic voltammetric studies

The redox properties of the complexes were studied in acetonitrile and dimethyl sulfoxide. The use of DMSO as solvent improved the solubility of the complexes but unfortunately, owing to the solvent cut-off, the potential range at positive potentials was only up to about 1 V. The relevant electrochemical data are summarised in Tables 3 and 4. Also listed in Table 3 are redox potentials of some ruthenium(II) mono-, bis- and tris-(2,2′-bipyridine) complexes as reference.

All the measured ruthenium complexes were in oxidation state II. At positive potentials, cyclic voltammograms revealed electrochemically reversible metal-based Ru^{II}–Ru^{III} oxidations. As can be seen in Tables 3 and 4, the expected and well known dependence of the metal-based oxidation potential on the electron acceptor or donor nature of the attached ligand is clearly observed.[2] Introduction of electron-withdrawing CO_2H groups to 2,2′-bipyridine shifts the potential of the redox couple to more positive values. This trend is best seen with bis- and tris-(bipyridine) complexes, where the potential values ($E_{1/2}$) vary from −0.06 to 0.19 V and from 0.91 to 1.37 V, correspondingly. Thus, carboxylic acid groups readily remove electron density from the ruthenium centre *via* the bipyridine ring, rendering the Ru^{II}–Ru^{III} oxidation more difficult. Moreover, ruthenium metal is more difficult to oxidise in $Ru(H_2dcbpy)_2(NCS)_2$ than in $Ru(H_2dcbpy)_2X_2$ (X = Cl or Br), which is seen as a positive shift (*ca.* 400 mV in DMSO) in potential. This behaviour emphasises the stronger π-acceptor character of co-ordinated thiocyanate compared to halide ligands. Overall, the measured oxidation potentials correlated well with earlier published results with one exception. Complexes **2** and **3** did not show any sign of metal centred oxidation in acetonitrile at the expected potential range (see Table 3). This is related to the poor solubility of **2** and **3** in CH_3CN because Ru^{II}–Ru^{III} peak systems are seen in DMSO. Furthermore, ethanol was used as solvent in the literature.[18]

The electrochemical behaviour of $Ru^{II}(H_2dcbpy)$ complexes at negative potentials has been studied less. This is partly due to the fact that understanding the redox behaviour of the sensitiser *cis*-$Ru(H_2dcbpy)_2(NCS)_2$ at positive potentials is essential for the functioning of dye sensitised solar cells.[20] Even if the redox reactions are complicated we have tried to clarify further the voltammetric characteristics of the $Ru^{II}(H_2dcbpy)$ complexes at negative potentials. The electrochemical reactions that took place were mainly ligand-based reductions. In general, these reactions were irreversible (see Tables 3 and 4) and redox

Table 1 Selected bond lengths and O···O distances (Å) of hydrogen bonds for Ru(H_2dcbpy)(CO)$_2$Cl$_2$·H_2O **1**, Ru(H_2dcbpy)$_2$Br$_2$·H_2O **3**, Ru(H_2dcbpy)$_2$(dcbpy)·6H_2O **4** and [Ru(H_2dcbpy)$_3$]Cl$_2$·2$\frac{3}{4}$$H_2O$ **5**

	1	**3**	**4**	**5A**	**5B**
Ru(1)–Cl(1)[a]	2.4205(11)	2.5436(4)			
Ru(1)–Cl(2)[b]	2.3722(11)	2.5650(4)			
Ru(1)–C(1)	1.937(5)				
Ru(1)–C(3)	1.873(5)				
Ru(1)–N(1)	2.121(3)	2.009(2)	2.047(4)	2.060(2)	2.065(2)
Ru(1)–N(2)	2.084(3)	2.048(2)	2.045(4)	2.072(2)	2.060(2)
Ru(1)–N(3)		2.029(2)	2.062(4)	2.059(2)	2.049(2)
Ru(1)–N(4)		2.047(2)	2.067(4)	2.056(2)	2.047(2)
Ru(1)–N(5)			2.056(4)	2.054(2)	2.043(2)
Ru(1)–N(6)			2.060(4)	2.052(2)	2.076(2)
C(1)–O(1)	1.040(5)				
C(3)–O(3)	1.116(4)				
C(40)–O(40)	1.304(5)	1.316(3)	1.319(6)	1.321(4)	1.308(3)
C(40)–O(41)	1.211(5)	1.209(3)	1.209(6)	1.205(4)	1.218(3)
C(50)–O(50)		1.327(4)	1.305(6)	1.325(4)	1.322(3)
C(50)–O(51)		1.187(4)	1.193(6)	1.210(4)	1.209(3)
C(60)–O(60)		1.313(4)	1.259(6)	1.322(3)	1.331(3)
C(60)–O(61)		1.197(4)	1.266(6)	1.197(3)	1.207(3)
C(70)–O(70)		1.321(4)	1.272(7)	1.334(3)	1.309(3)
C(70)–O(71)		1.205(4)	1.237(7)	1.200(3)	1.230(3)
C(80)–O(80)			1.258(6)	1.324(3)	1.323(4)
C(80)–O(81)			1.232(6)	1.204(3)	1.197(4)
C(90)–O(90)			1.258(7)	1.210(3)	1.326(4)
C(90)–O(91)			1.249(6)	1.312(3)	1.206(4)

Hydrogen bond[c]	**1**		**4**	Hydrogen bond[d]	**5**
O(40)···O(94)	2.663(5)		2.531(5)	O(40)···Cl(1)	3.043(2)
O(60)···O(95)			2.785(6)	O(90)···Cl(2)	3.001(2)
O(61)···O(98)			2.686(6)	O(61)···O(98)	2.546(3)
O(71)···O(99)			2.807(6)	O(40B)···Cl(2)	2.979(2)
O(81)···O(97)			2.824(6)	O(70B)···Cl(3)	3.014(2)
O(90)···O(96)			2.730(5)	O(80B)···O(97)	2.532(2)
O(91)···O(50)				O(90B)···Cl(4)	2.9766(19)

Oxygens ≥94 are due to water molecules. [a] Br(1) in complex **3**. [b] Br(2) in **3**. [c] For **1** and **4**. [d] For **5**.

Table 2 Selected bond angles (°) for complexes **1**, **3**, **4** and **5**

	1	**3**	**4**	**5A**	**5B**
N(1)–Ru(1)–N(2)	78.64(12)	79.08(9)	78.55(15)	78.44(8)	79.20(8)
N(3)–Ru(1)–N(4)		78.96(9)	78.82(15)	78.72(8)	78.63(8)
N(5)–Ru(1)–N(6)			79.11(15)	78.54(8)	78.52(8)
N(1)–Ru(1)–N(4)		95.46(9)	175.07(15)	177.83(9)	173.45(8)
N(2)–Ru(1)–N(5)[a]		173.45(9)	174.85(15)	175.97(9)	178.07(9)
N(3)–Ru(1)–N(6)			174.17(15)	174.11(8)	175.39(8)
N(1)–Ru(1)–C(1)[b]	177.49(14)	173.61(6)			
N(2)–Ru(1)–Cl(2)[c]	171.85(9)	174.07(6)			
Cl(1)–Ru(1)–C(3)	178.68(12)				
Ru(1)–C(1)–O(1)	174.9(4)				
Ru(1)–C(3)–O(3)	176.0(3)				
O(40)–C(40)–O(41)	125.1(4)	122.9(3)	125.1(5)	125.0(3)	125.2(2)
O(50)–C(40)–O(51)	125.4(4)	123.7(3)	126.4(5)	124.4(2)	125.1(3)
O(60)–C(40)–O(61)		123.5(3)	124.9(5)	125.6(2)	125.3(2)
O(70)–C(40)–O(71)		124.6(3)	126.3(5)	118.1(2)	123.2(2)
O(80)–C(40)–O(81)			126.5(5)	125.3(2)	124.6(3)
O(90)–C(40)–O(91)			125.8(5)	125.0(2)	124.0(2)

[a] N(2)–Ru(1)–N(4) for complex **3**. [b] N(1)–Ru(1)–Br(1) for **3**. [c] N(3)–Ru(1)–Br(2) for **3**.

potentials varied from −0.86 (**5**) to −2.20 V (**2**) *vs.* Ag^+–Ag reference electrode. It is clearly seen that the electron-withdrawing H_2dcbpy ligands result in redox potentials at more positive values. The shapes of the cyclic voltammograms in the two solvents were about the same, although the peaks were more distinct in DMSO due to better solubility.

In the reduction of ruthenium(II) polypyridine complexes the extra electron is added to the lowest unoccupied molecular orbital (LUMO), usually a π* orbital of a polypyridine ligand.[21,22] Each bipyridine ligand accepts two electrons in its LUMO during the reduction of ruthenium(II) bipyridine compounds.[23] Hence it is expected that several reductive waves could be observed in the cyclic voltammograms. If we now consider the Ru(H_2dcbpy) complexes **1**–**5**, one to three reductive waves were observed at the used potential range from 0 to −2.3 V. In acetonitrile, all the complexes exhibited only one detectable *irreversible* reduction [E_{pc} from −1.47 (**1**) to −1.57 V (**2**,**3**)], whereas in dimethyl sulfoxide *irreversible* [E_{pc} from −1.37 (**1**) to −1.48 V (**3**)] and *reversible* [$E_{1/2}$ from −1.85 (**2**,**4**,**5**) to −1.99 V (**4**)] reduction waves were found at a platinum working electrode. Interestingly, the more positive reductions all are irreversible in nature. It is known that the reduced form of ruthenium(II)

Table 3 Redox potentials (V) for selected $Ru^{II}(L)$ complexes [L = H_2dcbpy, bpy or dmbpy (dmbpy = 4,4′-dimethyl-2,2′-bipyridine)] in CH_3CN

	$Ru^{2+/3+}$	Ligand localised redox reactions		
Compound	$E_{\frac{1}{2}}{}^{a}$	$E_{pc}{}^{b}$	$E_{pa}{}^{b}$	Ref.
$Ru(H_2dcbpy)(CO)_2Cl_2$ **1**	1.62	−1.47	—	[c]
$Ru(bpy)(CO)_2Cl_2$	1.47	−1.58	−0.69	11(*b*)
$Ru(dmbpy)(CO)_2Cl_2$	1.41	−1.62	−0.85	11(*b*)
$Ru(H_2dcbpy)_2Cl_2$ **2**	[d]	−1.57	−1.21	[c]
$Ru(H_2dcbpy)_2Br_2$ **3**	[d]	−1.57	−1.02	[c]
$Ru(H_2dcbpy)_2(NCS)_2$	0.55	−1.10	—	[c]
$Ru(H_2dcbpy)_2(NCS)_2{}^{e}$	0.47	[f]	[f]	18
$Ru(H_2dcbpy)_2Cl_2{}^{e}$	0.19[g]	[f]	[f]	18
$Ru(bpy)_2Cl_2{}^{e}$	−0.06	−1.99,[a] −2.24[a]	—	2(*k*)
$Ru(H_2dcbpy)_2(dcbpy)$ **4**	1.37	−1.55	—	[c]
$Ru(H_2dcbpy)_3{}^{2+}$ **5**	[d]	−1.53	−1.04	[c]
$Ru(bpy)_3{}^{2+\,e}$	0.91	−1.71,[a] −1.90,[a] −2.16[a]	—	2(*o*)
H_2dcbpy	—	−1.54	−0.86	[c]

[a] For the reversible wave, $E_{\frac{1}{2}} = \frac{1}{2}(E_{pa} + E_{pc})$. [b] E_{pc} and E_{pa} are the peak potentials for the reductive and oxidative waves. [c] This work. [d] Not observed. [e] Potentials corrected *vs.* Ag^+–Ag reference electrode.[19] [f] Values not reported. [g] Measured in ethanol.

Table 4 Redox potentials (V) for $Ru^{II}(H_2dcbpy)$ complexes in DMSO

		$Ru^{2+/3+}$	Ligand localised redox reactions			
	Compound	$E_{\frac{1}{2}}{}^{a,b}$	$E_{pc}{}^{b,c}$	$E_{pa}{}^{b,c}$	$E_{pc}{}^{c,d}$	$E_{pa}{}^{c,d}$
1	$Ru(H_2dcbpy)(CO)_2Cl_2$	[e]	−1.37, −1.75	—	−1.88, −2.18	−2.01
2	$Ru(H_2dcbpy)_2Cl_2$	0.15	−1.47, −1.85[a]	−0.91	−1.94, −2.20	—
3	$Ru(H_2dcbpy)_2Br_2$	0.23	−1.48, −1.75	−0.89	−1.96, −2.17	—
	$Ru(H_2dcbpy)_2(NCS)_2$	0.59[f]	−0.94, −1.55	−0.89	[g]	[g]
4	$Ru(H_2dcbpy)_2(dcbpy)$	[e]	−1.38, −1.85,[a] −1.99[a]	−0.90	−1.75	—
5	$Ru(H_2dcbpy)_3{}^{2+}$	[e]	−1.53, −1.85,[a] −1.98[a]	−0.86	−2.01	—
	H_2dcbpy	—	−1.45	−0.93	[g]	[g]

[a] For the reversible wave, $E_{\frac{1}{2}} = \frac{1}{2}(E_{pa} + E_{pc})$. [b] Measured at platinum working electrode. [c] E_{pc} and E_{pa} are the peak potentials for the reductive and oxidative waves. [d] Measured at GC working electrode. [e] Not observed due to the solvent cut-off. [f] Irreversible E_{pa} value. [g] Not measured.

polypyridine complexes is inert and usually the ligand-based reductions are reversible.[22] Furthermore, some electrochemical data for the mixed ligand complexes $[Ru(bpy)_2(L)]^{2+}$, where L = 3,3′-, 4,4′- or 5,5′-H_2dcbpy, have recently been reported.[24] The potential values ($E_{1/2}$) for reductions varied from −1.82 to −1.91 V. These were proposed to correspond to the reduction of bpy in the carboxylic acid containing H_2dcbpy ligand. Thus, the most negative reversible reactions of **1**–**5** can be assigned as bipyridine-based one-electron reductions.

The origin of the above-mentioned irreversible reductions is linked to the electrochemical behaviour of the carboxylic acid groups located in 4,4′ position in the 2,2′-bipyridine ring. During the scan to negative potentials at a platinum electrode one clear irreversible reduction peak was found in both solvents at the appropriate potential (see Tables 3 and 4). It is known that carboxylic acids can electrochemically be reduced according to reaction (1).[25] Thus, the first irreversible reductions with

$$CO_2H + e^- \longrightarrow CO_2{}^- + \tfrac{1}{2}H_2 \qquad (1)$$

complexes **1**–**5** correspond to the evolution of hydrogen. During the scan back to positive values the anodic peaks indicate the oxidation of liberated hydrogen, which can be seen at a platinum electrode.[25] The evolution of hydrogen was also observed as bubbles at the surface of the platinum electrode. It has recently been reported that *cis*-$Ru(H_2dcbpy)_2(NCS)_2$ **6** undergoes deprotonation by electrochemical reduction at platinum and glassy carbon electrodes. It was concluded that partial deprotonation of carboxylic acid groups is the most likely reaction, which may proceed through several routes resulting in $[Ru(Hdcbpy^-)_2(NCS)_2]^{2-}$ as principal product. Furthermore, cyclic voltammetry experiments revealed the complex nature of reductions at platinum compared to glassy carbon. This behaviour was connected with the lower overpotential for hydrogen gas formation at a platinum electrode.[26]

We have performed cyclic voltammetry experiments for complexes **1**–**5** at platinum and glassy carbon (GC) electrodes in DMSO. The same kind of voltammetric behaviour was observed for all the complexes as reported before.[26] The measured voltammograms were more complex and irreversible at platinum than at a glassy carbon electrode. It is clearly seen from the data in Table 4 that the characteristic peaks for hydrogen forming and oxidation of liberated hydrogen are not observed at a GC electrode. This is a consequence of hydrogen formation being suppressed at the GC electrode.

It can be concluded from the structures of the studied complexes (Figs. 1–3) that carboxylic acids are the easiest functional groups to reduce. In **1**–**3**, all the other ligands are stronger π acceptors. In **4** there are two H_2dcbpy ligands *vs.* one strongly negative carboxylate (dcbpy) ligand, whereas in **5** all three H_2dcbpy groups are electrochemically equivalent. The nature of the reduced species was not explicitly determined, but autoprotonation reactions of formed species may take place[27] as well as the formation of salts with the supporting electrolyte, tetrabutylammonium perchlorate. The reductive behaviour of carboxylic acid groups was investigated with benzoic acid in both solvents. This aromatic carboxylic acid revealed the same kind of cyclic voltammetry as free H_2dcbpy ($E_{pc} = -1.42$ V, $E_{pa} = -0.91$ V in CH_3CN; $E_{pc} = -1.55$ V, $E_{pa} = -0.98$ V in DMSO). Furthermore, the electrochemical reactions of the non-co-ordinating H_2dcbpy ligand were clearly found in voltammograms of the complexes. These experimental results strongly suggest that deprotonation of H_2dcbpy ligands causes the irreversible reductions and voltammetric characteristics which are observed at a platinum electrode.

There were two electrochemical phenomena occurring at negative potential, which are closely related to ligand-based reductions. First, the characteristic feature of the electrochemical behaviour of H_2dcbpy complexes (especially for **4** and

Table 5 UV-Vis absorption data for the Ru^{II}(H$_2$dcbpy) complexes in CH$_3$CN and Ru^{III}–Ru^{II} oxidation potentials (E_{calc}) calculated by using Lever's E(L) parameters

Starting complex	λ_{abs}/nm [a]	 [b]	E_{calc}[c]/V	E_{obs}/V
1	372	584, 454	0.89	0.88
2	560, 405	480	—	[d]
3	577, 438	584, 484	0.86	0.82
4	503	608, 466, 402	—	0.88
5	483	475, 406	0.84	0.86

[a] Before photoirradiation. [b] After photoirradiation. [c] Calculated from $E_{calc} = xE_L(X) + yE_L(Y) + zE_L(Z)$ for RuX$_x$Y$_y$Z$_z$ [3b] for the suggested photolysis products. [d] Irreversible oxidation.

5) in both solvents is the appearance of the same kind of cyclic voltammograms as with H$_2$dcbpy ligand itself. The second phenomenon is related to the reduction of the mono(H$_2$dcbpy) complex **1**. It has been reported earlier[28] that the electrochemical behaviour of mono(bipyridine) complexes, Ru(L)(CO)$_2$Cl$_2$ (L = bpy or dmbpy), at negative potentials is mainly governed by the formation and reactions of polymeric [{Ru(L)(CO)$_2$}$_n$] film. During a reductive scan to negative potentials ($E < -1.5$ V) the working electrode becomes covered with a dark film, which is then oxidatively fractured at potentials > -1.0 V. These reductive and oxidative reactions can be seen in cyclic voltammograms as strong, irreversible cathodic and anodic peaks, respectively. We found in our studies, however, that a polymeric film [{Ru(H$_2$dcbpy)(CO)$_2$}$_n$] was not formed in the reduction of Ru(H$_2$dcbpy)(CO)$_2$Cl$_2$. This distinctive behaviour can be explained by the electrochemical reduction of carboxylic acid groups. As mentioned, the film formation starts at potentials more negative than -1.5 V. This value is located approximately in the same potential range where the reduction of CO$_2$H groups takes place. We noted in our experiments the presence of a dark precipitate near the surface of the working electrode. Thus, the evolution of hydrogen and formation of other reduction products clearly prevent the attaching of polymer film to the surface of the platinum electrode.

Photochemistry

The photochemical behaviour of the Ru^{II}(H$_2$dcbpy) complexes **1**–**5** was studied under irradiation in acetonitrile solutions. Photolysis of Ru(L)(CO)$_2$Cl$_2$ (L = bpy or dmbpy) has been reported to produce three new complexes, where both the carbonyl and one of the chloride ligands is photosubstituted in three successive steps by a solvent molecule acetonitrile.[11] We carried out photolysis experiments to determine whether similar photosubstitution occurs with complexes **1**–**5**. The UV-Vis absorptions are presented in Table 5.

It has been found earlier that after photoirradiation of mono(bpy) complexes Ru(L)(CO)$_2$Cl$_2$ (L = bpy or dmbpy), the reversible Ru^{II}–Ru^{III} oxidation wave has moved to more negative potentials ($E_{1/2}$ = 0.74–0.78 V).[11] The change in oxidation potential is due to the formation of a mono-acetonitrile complex, Ru(L)(CO)(CH$_3$CN)Cl$_2$, in which the removal of one π-accepting CO ligand makes the ruthenium-oxidation easier. Upon photolysis of Ru(H$_2$dcbpy)(CO)$_2$Cl$_2$ **1** the acetonitrile solution changed from yellow to orange-red. At the same time the initial CO bands (ν_{CO} 2067 and 2006 cm^{-1}) disappeared and a new peak appeared at 1975 cm^{-1}. Cyclic voltammograms measured directly on the photolysis solution revealed the formation of a new reversible peak system ($E_{1/2}$ = 0.88 V; ΔE_p = 70 mV) for the oxidation of ruthenium located at a more positive value compared to that of Ru(bpy)(CO)(CH$_3$CN)Cl$_2$ because of the electron-withdrawing H$_2$dcbpy ligands. During a scan to negative potentials the above-mentioned H$_2$dcbpy-based reductions were observed ($E_{pc} = -1.41$ V and $E_{1/2} = -1.98$ V) corresponding to deprotonation of CO$_2$H groups and reduction of dcbpy ligand, respectively. The observed IR and UV-Vis spectra in CV experiments are in good agreement with previously published photolysis results for ruthenium(II) bpy complexes.[11] Thus the data suggest the formation of Ru(H$_2$dcbpy)(CO)(CH$_3$CN)Cl$_2$ as principal photolysis product.

The complexes Ru(H$_2$dcbpy)$_2$Cl$_2$ **2** and Ru(H$_2$dcbpy)$_2$Br$_2$ **3** behaved differently upon photoirradiation. For **2** the initial acetonitrile solution changed from purple-red to almost colourless and at the same time a dark red precipitation was formed. On the contrary, the solution of **3** changed from pale to dark red. The UV-Vis absorptions are seen at Table 5. These changes in colours are thus indicating ongoing light-induced chemical reactions. Photochemical reactions of corresponding bis(bipyridine) ligated complexes have extensively been studied. It is known that photoreactions especially in co-ordinating solvents (solv) proceed according to reactions (2) and (3), where X and Y are monodentate ligands.[9b,10a] It could be assumed that reactions (2) and (3) are valid also during photoirradiation of Ru(H$_2$dcbpy)$_2$Cl$_2$ and Ru(H$_2$dcbpy)$_2$Br$_2$.

$$\mathrm{Ru(bpy)_2XY}^{n+} + \mathrm{solv} \xrightarrow{h\nu} \mathrm{Ru(bpy)_2Y(solv)}^{p+} + \mathrm{X} \quad (2)$$

$$\mathrm{Ru(bpy)_2Y(solv)}^{p+} + \mathrm{solv} \xrightarrow{h\nu} \mathrm{Ru(bpy)_2(solv)_2}^{q+} + \mathrm{Y} \quad (3)$$

According to the above results, we would expect the formation of [Ru(H$_2$dcbpy)$_2$(CH$_3$CN)X]$^+$ (X = Cl or Br) and [Ru(H$_2$dcbpy)$_2$(CH$_3$CN)$_2$]$^{2+}$ upon photoirradiation of complexes **2** and **3** in CH$_3$CN. The cyclic voltammograms measured directly from the photolysis solutions resulted in suggestions about light-induced ligand substitution reactions. At positive potentials a new irreversible peak appeared (E_{pa} = 1.10 V) for **2** whereas a reversible peak system ($E_{1/2}$ = 0.82 V; ΔE_p = 61 mV) was found for **3**. Furthermore, at negative potentials irreversible ligand-based reductions are observed ($E_{pc} = -1.16$ V; $E_{pa} = -0.84$ V for **2** and $E_{pc} = -1.51$ V for **3**). If these potential values are compared to the original values (Table 3) it is noticed that the redox reactions occur at more positive potentials. Thus the reduction of H$_2$dcbpy ligands is easier and it can be concluded that changes have taken place in the ruthenium-co-ordination sphere. The most probable reason for this is the light-induced photosubstitution of halide ligands with solvent CH$_3$CN. Further evidence for this conclusion is found when calculated oxidation potentials (by using Lever's ligand electrochemical parameters) are compared to observed values (see Table 5). For the reversible wave systems of **3** the correlation was good but E(L) could not been applied to the irreversible peaks of **2**.

Upon photoirradiation an acetonitrile solution of complex **4** changed from pale yellow to dark red and of **5** from orange to orange-red. At positive potentials almost reversible one-electron wave systems ($E_{1/2}$ = 0.88 V, ΔE_p = 96 mV for **4**; $E_{1/2}$ = 0.86 V, ΔE_p = 50 mV for **5**) were formed. At negative potentials, the observed peak systems exhibited the same kind of reductive behaviour as the above-mentioned photolysed solutions of **2** and **3**. It has been reported,[8b] that under appropriate conditions photolysis of Ru(bpy)$_3$$^{2+}$ results in loss of bpy ligand. Furthermore, in acetonitrile solutions, the formation of CH$_3$CN co-ordinated ruthenium bis(bpy) complexes originating from [Ru(bpy)$_3$]Cl$_2$ has been found to occur.[8c] Therefore photosubstitution reactions of **4** and **5** to give the corresponding bis(H$_2$dcbpy) complex are possible. The wave systems at positive potentials can then be due to Ru^{II}–Ru^{III} oxidation, because in general the substitution of one bpy ligand in Ru(bpy)$_3$$^{2+}$ makes the metal-based oxidation much more easier (see Tables 3 and 4).

The products of photoirradiation were further characterised by using Lever's E(L) parameters to show that the Ru^{II}–Ru^{III}

oxidation potentials were reasonable. The values of E(L) for a selected ligand were taken from the literature[3b] except for H_2dcbpy ligand. The E(H_2dcbpy) value was experimentally fitted to +0.35 V by using the starting complexes **1**–**5** as reference material. Experimental values shown in Table 5 are closely correlated with calculated potentials for complexes **1**, **3** and **5**. According to the E_{calc} values, the most likely photolysis products are Ru(H_2dcbpy)(CO)(CH_3CN)Cl_2 for **1** and [Ru(H_2dcbpy)$_2$(CH_3CN)X]$^+$ (X = Br **3** or Cl **5**). The photoirradiation of **2** produces probably the same product as **3** even if the E_{calc} could not be calculated. The voltammetric and UV-Vis data collected after photoirradiation supported the formation of [Ru(H_2dcbpy)$_2$(CH_3CN)Cl]$^+$. The photolysis products of Ru(H_2dcbpy)$_2$(dcbpy) **4** could not be assigned by using Lever's parameters. Nevertheless, based on CV and UV-Vis data, [Ru(H_2dcbpy)$_2$(CH_3CN)$_2$]$^{2+}$ can be expected to be the main product but the formation of mixtures cannot completely be excluded.

Experimental

Materials

All reagents were p.a. grade used without further purification. $RuCl_3 \cdot 3H_2O$ and [Ru(CO)$_3$Cl$_2$]$_2$ were obtained from Alfa and 2,2′-bipyridine-4,4′-dicarboxylic acid from Fluka. Methanol (Riedel-de Haën), HCl (37%, Riedel-de Haën) and HBr (47%, Merck) were used as received.

Syntheses

***trans*(Cl)- and *cis*(CO),*cis*(Cl)-Ru(H_2dcbpy)(CO)$_2$Cl$_2$ 1.** $Ru_3(CO)_{12}$ (264 mg, 0.4 mmol), H_2dcbpy (101 mg, 0.4 mmol), concentrated HCl (2.5 ml) and water (0.5 ml) were placed in a 60 ml Berghof digestive pressure bomb with a poly(tetrafluoroethylene) (PTFE) liner. The reaction system was heated for 3 h at 200 °C and slowly cooled to room temperature. The precipitated greenish yellow solid product (110 mg) was filtered off and washed several times with water to remove HCl. Calc. for Ru(H_2dcbpy)(CO)$_2$Cl$_2$: C, 35.6; N, 5.9; H, 1.7. Found: C, 35.5; N, 5.8; H, 1.7%. IR (in CH_3OH): ν(CO) 2071vs cm^{-1}, 2009vs and 1737 (br) m cm^{-1}. ^{13}C-{^{1}H} NMR (in d_6-DMSO): for bpy, δ 158.9, 158.5, 146.3, 131.3 and 128.1 (all singlets); for CO_2H, δ 168.6 (singlet); for CO, δ 200.2 (singlet).

***trans*(Cl)-Ru(H_2dcbpy)(CO)$_2$Cl$_2$ 1.** 100 mg [Ru(CO)$_3$Cl$_2$]$_2$ and 50 mg H_2dcbpy were placed in a pressure vessel in solution with 1 ml HCl (37%) and 2 ml water. The mixture was heated at 200 °C for 3 hours. A greenish yellow product was filtered off and washed with water. Found: C, 35.4; N, 5.9; H, 1.8%. ^{1}H NMR spectrum of dried *trans*(Cl)-Ru(H_2dcbpy)(CO)$_2$Cl$_2$ was measured in d_6-DMSO: for bpy, δ 9.45 (d), 9.21 (s) and 8.22 (d); for CO_2H, not distinguishable. ^{13}C-{^{1}H} NMR (in d_6-DMSO): for bpy, δ 158.9, 158.5, 146.3, 131.3 and 128.1 (all singlets); for CO_2H, δ 168.6 (singlet); for CO, δ 200.2 (singlet). *cis*(CO),*cis*(Cl)-Ru(H_2dcbpy)(CO)$_2$Cl$_2$ was crystallised from methanol–water solution and the crystal structure determined by X-ray diffraction.

Ru(H_2dcbpy)$_2$Cl$_2$ 2. $RuCl_3 \cdot 3H_2O$ (50 mg), H_2dcbpy (93 mg), 1.5 ml HCl (37%) and 1.5 ml water were added in a reaction vessel. The temperature was raised to 200 °C and maintained for 4 hours. After slow cooling period (10 °C h^{-1}) black crystals were filtered off and washed with water and methanol. The dried product was characterised by X-ray crystallography and elemental analysis. Calc. for Ru(H_2dcbpy)$_2$Cl$_2 \cdot H_2O$: C, 42.5; N, 8.3; H, 2.7. Found: C, 42.5; N, 8.3; H, 2.7.

Ru(H_2dcbpy)$_2$Br$_2$ 3. 50 mg of $RuCl_3 \cdot 3H_2O$ and 93 mg H_2dcbpy were weighed in a pressure bomb. A solution of 2 ml HBr/ 2 ml water was added and the mixture heated at 200 °C for 6 h. After slow cooling (5 °C h^{-1}) the dark brown product was filtered off and washed with water. The dried product was characterised by X-ray crystallography and elemental analysis. Calc. for Ru(H_2dcbpy)$_2$Br$_2 \cdot H_2O$: C, 37.6; N, 7.3; H, 2.4. Found: C, 37.5; N, 7.3; H, 2.2.%

Ru(H_2dcbpy)$_2$(dcbpy) 4. $RuCl_3 \cdot 3H_2O$ (50 mg, 0.19 mmol), H_2dcbpy (140 mg, 0.57 mmol) and 2 ml water were added to a Berghof autoclave. The temperature was raised to 220 °C and maintained for 3 hours. After slow cooling (10 °C h^{-1}), dark red crystals were filtered out and washed with water and methanol. The dried product was characterised by X-ray crystallography and elemental analysis. Calc. for [Ru(H_2dcbpy)$_2$(dcbpy)]$\cdot 6H_2O$: C, 46.4; N, 9.0; H, 2.9. Found: C, 46.2; N, 9.1, H, 3.0%.

[Ru(H_2dcbpy)$_3$]Cl$_2$ 5. $RuCl_3 \cdot 3H_2O$ (50 mg) and H_2dcbpy (140 mg) were placed in a Berghof digestive pressure bomb, where 1 ml of HCl and 2 ml of water were added. The mixture was heated at 200 °C for 3 h 30 min and cooled very slowly (3 °C h^{-1}) to room temperature. The dark red (nearly black) precipitate was filtered off and washed a few times with water. The air-dried product consisted of dark red [Ru(H_2dcbpy)$_3$]$^{2+}$(Cl$^-$)$_2 \cdot$ 2¾(H_2O) crystals. Calc. for [Ru(H_2dcbpy)$_3$]Cl$_2$: C, 47.8; N, 9.3; H, 2.7. Found: C, 47.5; N, 9.2, H, 2.9%.

X-ray Crystallography

X-Ray diffraction data were collected with a Nonius Kappa-CCD diffractometer using Mo-Kα radiation (λ = 0.71073 Å). Denzo and Scalepack[29] programs were used for cell refinements and data reduction. The structures were solved by direct methods with SHELXS 97.[30] Structure refinements were carried out with SHELXL 97.[31] Structure **5** was solved as a racemic twin in the non-centrosymmetric space group *Cc* (refined absolute structure parameter 0.272(11)). The asymmetric unit consists of two ruthenium units, [Ru(H_2dcbpy)$_3$]$^{2+}$, four Cl$^-$ counter anions and 5½ water molecules. Solution of **5** in centrosymmetric space group *C*2/*c* was not satisfactory. All aromatic hydrogens were placed in idealised positions. In **1** and **4**, hydrogens of the carboxylate groups were located from the Fourier difference map and refined with fixed thermal parameter $U_{iso} = 0.06$ Å^2. In **1** also the water hydrogens were refined, with $U_{iso} = 0.08$ Å^2. In **3**–**5** hydrogens of the water molecules, and in **3** and **5** CO_2H hydrogens, were located from the Fourier difference map but not refined. Carboxylate groups in **1**, **3** and **5** were in protonated, neutral form. Two of the carboxylate groups in Ru(H_2dcbpy)$_2$(dcbpy) **4** were in non-protonated, ionic form compensating the positive charge on the Ru^{2+}. The non-protonated carboxylates formed a strong hydrogen bond interaction with protonated CO_2H groups of a neighbouring molecule with O···O distances of 2.474(6) and 2.420(5) Å. In one of the protonated carboxylates OH and =O groups were disordered, giving almost equal C–O distances of 1.259(6) and 1.266(6) Å. Only one of the possible hydrogen positions of this disordered moiety was located from the Fourier difference map. The hydrogen was fixed on this position. Both oxygens of the disordered group formed hydrogen bonds with water molecules [O···O 2.785(6) and 2.686(6) Å]. In Ru(H_2dcbpy)$_2$Br$_2 \cdot H_2O$ **3** the water molecule was disordered in two positions with population parameters 0.45/0.55. Crystallographic data are summarised in Table 6.

CCDC reference number 186/2041.

See http://www.rsc.org/suppdata/dt/b0/b004751l/ for crystallographic files in .cif format.

Spectroscopic studies

Infrared spectra were measured with Nicolet Magna 750 and Nicolet Impact 400D FTIR spectrometers, ^{1}H and ^{13}C NMR spectra on a Bruker AMX 400 (400 MHz) spectrometer

Table 6 Crystallographic data for $Ru(H_2dcbpy)(CO)_2Cl_2{\cdot}H_2O$ **1**, $Ru(H_2dcbpy)_2Br_2{\cdot}H_2O$ **3**, $Ru(H_2dcbpy)_2(dcbpy){\cdot}6H_2O$ **4** and $[Ru(H_2dcbpy)_3]Cl_2{\cdot}2\frac{3}{4}H_2O$ **5**

	1	**3**	**4**	**5**
Chemical formula	$C_{14}H_{10}Cl_2N_2O_7Ru$	$C_{24}H_{17}Br_2N_4O_9Ru$	$C_{36}H_{34}N_6O_{18}Ru$	$C_{36}H_{29.50}Cl_2N_6O_{14.75}Ru$
M	490.21	766.31	939.76	954.13
Crystal system	Monoclinic	Monoclinic	Monoclinic	Monoclinic
Space group	$P2_1/c$	$P2_1/n$	$P2_1/c$	Cc
a/Å	8.1339(2)	12.1882(2)	10.1410(2)	22.1485(3)
b/Å	15.9462(5)	11.27370(10)	18.2804(6)	18.7892(3)
c/Å	13.3650(4)	19.8150(3)	21.0357(7)	21.4865(2)
β/°	95.520(2)	106.0100(10)	100.988(2)	118.5930(10)
V/Å^3	1725.47(9)	2617.10(6)	3828.01(19)	7851.15(18)
T/K	293(2)	293(2)	120(2)	150(2)
Z	4	4	4	8
μ/mm^{-1}	1.259	3.714	0.499	0.614
No. reflections collected	11496	9196	12543	51929
No. unique reflections	3028	4730	6383	17064
R_{int}	0.0759	0.0138	0.0384	0.0290
$R1$	0.0380	0.0274	0.0458	0.0249
$wR2$	0.0630	0.0663	0.1069	0.0624

and UV-Vis spectra on a Shimadzu UV-240 spectrometer. Elemental analyses were performed with an EA1110 CHNS-O (Carlo Erba Instruments) analyser.

Electrochemical instrumentation and procedure

Acetonitrile (Merck, p.a.), dimethyl sulfoxide (Merck, p.a.), and tetrabutylammonium perchlorate (TBAP) (Fluka, electrochemical grade) were used as received. Cyclic voltammetry was conducted with an Autolab PGSTAT20 potentiostat-galvanostat. Solutions for measurement in 0.1 M NBu_4ClO_4–CH_3CN or –DMSO were approximately 2 mM and before use were purged with argon in a three-electrode cell. In all measurements the working electrode was a platinum disk (Metrohm, area 1.28 cm^2) or a glassy carbon rod (Metrohm, area 0.97 cm^2), with a platinum wire (Metrohm, length 0.5 cm) or glassy carbon disk (Metrohm, area 0.28 cm^2) as the auxiliary electrode. The electrodes were polished with alumina and rinsed with distilled water and acetone before use. Potentials are referred to the Ag^+–Ag electrode (0.01 M $AgNO_3$ in CH_3CN). Under the experimental conditions the Fc^+–Fc (ferrocenium–ferrocene) couple potential was 0.01 V. In all experiments the potential scan rate was 100 mVs $^{-1}$.

Photochemical instrumentation

In photolysis experiments all samples were irradiated under argon with a 450 W Xe-discharge lamp equipped with IR filter (Oriel Model 8540). The photolysis cell was a water-cooled vessel with path length of 3 cm. All reactions were run in acetonitrile and their progress was monitored by IR and UV-Vis spectroscopy. For the cyclic voltammetry studies the resulting photolysis solutions were either evaporated to dryness and the residue dissolved in 0.1 M NBu_4ClO_4–CH_3CN solution or voltammograms were measured directly from the photolysis solutions.

Acknowledgements

Financial support of this work was provided by the Academy of Finland.

References

1 K. Kalyanasundaram, *Photosensitization and Photocatalysis Using Inorganic and Organometallic Compounds*, eds. K. Kalyanasundaram and M. Grätzel, Kluwer Academic Publishers, Dordrecht, 1993.

2 (*a*) B. P. Sullivan, D. J. Salmon and T. J. Meyer, *Inorg. Chem.*, 1978, **17**, 3334; (*b*) H. D. Abruña, T. J. Meyer and R. W. Murray, *Inorg. Chem.*, 1979, **18**, 3233; (*c*) B. P. Sullivan, D. J. Salmon, T. J. Meyer and J. Peedin, *Inorg. Chem.*, 1979, **18**, 3369; (*d*) P. Belser, A. Zelewsky and M. Zehnder, *Inorg. Chem.*, 1981, **20**, 3098; (*e*) A. H. Tinnemans, K. Timmer, M. Reinten, J. G. Kraaijkamp, A. H. Alberts, J. G. M. van der Linden, J. E. J. Schmitz and A. A. Saaman, *Inorg. Chem.*, 1981, **20**, 3698; (*f*) C. M. Elliott and E. J. Hershenhart, *J. Am. Chem. Soc.*, 1982, **104**, 7519; (*g*) J. L. Walsh and B. Durham, *Inorg. Chem.*, 1982, **21**, 329; (*h*) D. E. Morris, K. W. Hanck and M. K. DeArmond, *J. Am. Chem. Soc.*, 1983, **105**, 3032; (*i*) Y. Ohsawa, M.-H. Whangbo, K. W. Hanck and M. K. DeArmond, *Inorg. Chem.*, 1984, **23**, 3426; (*j*) B. P. Sullivan, J. V. Caspar, S. R. Johnson and T. J. Meyer, *Organometallics*, 1984, **3**, 1241; (*k*) B. P. Sullivan, D. Conrad and T. J. Meyer, *Inorg. Chem.*, 1985, **24**, 3640; (*l*) T. Matsumura-Inoue, I. Ikemoto and Y. Umezava, *J. Electroanal. Chem. Interfacial Electrochem.*, 1986, **209**, 135; (*m*) J. Ochmanska and P. G. Pickup, *Can. J. Chem.*, 1990, **69**, 653; (*n*) S. J. Slattery, N. Gokaldas, T. Mick and K. A. Goldsby, *Inorg. Chem.*, 1994, **33**, 3621; (*o*) P. A. Anderson, G. B. Deacon, K. H. Haarmann, F. R. Keene, T. J. Meyer, D. A. Reitsma, B. W. Skelton, G. F. Strouse, N. C. Thomas, J. A. Treadway and A. H. White, *Inorg. Chem.*, 1995, **34**, 6145; (*p*) J. A. Treadway and T. J. Meyer, *Inorg. Chem.*, 1999, **38**, 2267.

3 (*a*) E. S. Dodsworth and A. B. P. Lever, *Chem. Phys. Lett.*, 1986, **124**, 152; (*b*) A. B. P. Lever, *Inorg. Chem.*, 1990, **29**, 1271; (*c*) H. Masui, A. B. P. Lever and E. S. Dodsworth, *Inorg. Chem.*, 1993, **32**, 258.

4 M.-N. Collomb-Dunand-Sauthier, A. Deronzier and R. Ziessel, *J. Electroanal. Chem. Interfacial Electrochem.*, 1993, **350**, 43; *Inorg. Chem.*, 1994, **33**, 2961.

5 C. Caix-Cecillon, S. Chardon-Noblat, A. Deronzier, M. Haukka, T. A. Pakkanen, R. Ziessel and D. Zsoldos, *J. Electroanal. Chem. Interfacial Electrochem.*, 1999, **466**, 187.

6 T. J. Meyer, *Pure Appl. Chem.*, 1986, **58**, 1193; *Acc. Chem. Res.*, 1989, **22**, 163.

7 N. Sutin, *J. Photochem.*, 1979, **10**, 19.

8 (*a*) P. E. Hoggard and G. B. Porter, *J. Am. Chem. Soc.*, 1978, **100**, 1457; (*b*) R. F. Jones and D. J. Cole-Hamilton, *Inorg. Chim. Acta*, 1981, **53**, L3; (*c*) B. Durham, J. V. Caspar, J. K. Nagle and T. J. Meyer, *J. Am. Chem. Soc.*, 1982, **104**, 4803; (*d*) J. V. Caspar and T. J. Meyer, *J. Am. Chem. Soc.*, 1983, **105**, 5583.

9 (*a*) B. Durham, S. R. Wilson, D. J. Hodgson and T. J. Meyer, *J. Am. Chem. Soc.*, 1980, **102**, 600; (*b*) D. V. Pinnick and B. Durham, *Inorg. Chem.*, 1984, **23**, 1440.

10 (*a*) B. Durham, J. L. Walsh, C. L. Carter and T. J. Meyer, *Inorg. Chem.*, 1980, **19**, 860; (*b*) S. Gould, T. R. O'Toole and T. J. Meyer, *J. Am. Chem. Soc.*, 1990, **112**, 9490; (*c*) A.-C. Laemmel, J.-P. Collin and J.-P. Sauvage, *Eur. J. Inorg. Chem.*, 1999, 383.

11 (*a*) M.-N. Collomb-Dunand-Sauthier, A. Deronzier and R. Ziessel, *J. Organomet. Chem.*, 1993, **444**, 191; (*b*) E. Eskelinen, M. Haukka, T. Venäläinen, T. A. Pakkanen, M. Wasberg, S. Chardon-Noblat and A. Deronzier, *Organometallics*, 2000, **19**, 163.

12 G. B. Deacon, C. M. Kepert, N. Sahely, B. W. Skelton, L. Spiccia, N. C. Thomas and A. H. White, *J. Chem. Soc., Dalton Trans.*, 1999, 275.

13 (*a*) M. Haukka, J. Kiviaho, M. Ahlgrén and T. A. Pakkanen, *Organometallics*, 1995, **14**, 825; (*b*) P. Homanen, M. Haukka, T. A. Pakkanen, J. Pursiainen and R. H. Laitinen, *Organometallics*, 1996, **15**, 4081; (*c*) P. Homanen, M. Haukka, S. Luukkanen, M. Ahlgrén

and T. A. Pakkanen, *Eur. J. Inorg. Chem.*, 1999, 101; (*d*) M. Haukka, P. Hirva, S. Luukkanen, M. Kallinen, M. Ahlgrén and T. A. Pakkanen, *Inorg. Chem.*, 1999, **38**, 3182.
14 P. Homanen, M. Haukka, M. Ahlgrén and T. A. Pakkanen, *Inorg. Chem.*, 1997, **36**, 3794.
15 V. Shklover, Yu. E. Ovchinnikov, L. S. Braginsky, S. M. Zakeeruddin and M. Grätzel, *Chem. Mater.*, 1998, **10**, 2533.
16 M. Haukka, M. Ahlgrén and T. A. Pakkanen, *J. Chem. Soc.*, *Dalton Trans.*, 1996, 1927.
17 M. Haukka, T. Venäläinen, M. Ahlgrén and T. A. Pakkanen, *Inorg. Chem.*, 1995, **34**, 2931.
18 M. K. Nazeeruddin, A. Kay, I. Rodicio, R. Humphry-Baker, E. Müller, P. Liska, N. Vlachopoulos and M. Grätzel, *J. Am. Chem. Soc.*, 1993, **115**, 6382.
19 N. G. Connelly and W. E. Geiger, *Chem. Rev.*, 1996, **96**, 877.
20 A. M. Bond, G. B. Deacon, J. Howitt, D. R. MacFarlane, L. Spiccia and G. Wolfbauer, *J. Electrochem. Soc.*, 1999, **146**, 648.
21 R. D. Webster, A. M. Bond and T. Schmidt, *J. Chem. Soc.*, *Perkin Trans. 2*, 1995, 1365.
22 V. Balzani, A. Juris, M. Venturi, S. Campagna and S. Serroni, *Chem. Rev.*, 1996, **96**, 759.
23 N. Pramanik and S. Bhattacharya, *Polyhedron*, 1997, **16**, 1755.
24 P.-H. Xie, Y.-J. Hou, B.-W. Zhang, Y. Cao, F. Wu, W.-J. Tian and J.-C. Shen, *J. Chem. Soc.*, *Dalton Trans.*, 1999, 4217.
25 D. T. Sawyer, A. Sobkowiak and J. L. Roberts, Jr., *Electrochemistry for Chemists*, John Wiley & Sons, Inc., New York, 1995, chs. 8 and 12.
26 G. Wolfbauer, A. M. Bond, G. B. Deacon, D. R. MacFarlane and L. Spiccia, *J. Am. Chem. Soc.*, 2000, **122**, 130.
27 M. Aguilar-Martínez, G. Cuevas, M. Jiménez-Estrada, I. González, B. Lotina-Hennsen and N. Macías-Ruvalcaba, *J. Org. Chem.*, 1999, **64**, 3684.
28 S. Chardon-Noblat, A. Deronzier, R. Ziessel and D. Zsoldos, *Inorg. Chem.*, 1997, **36**, 5384.
29 Z. Otwinowski and W. Minor, *Methods Enzymol.*, 1997, **276**, 307.
30 G. M. Sheldrick, SHELXS 97, Program for Crystal Structure Determination, University of Göttingen, 1997.
31 G. M. Sheldrick, SHELXL 97, Program for Crystal Structure Refinement, University of Göttingen, 1997.